International Journal of Current Engineering and Technology
E-ISSN 2277 – 4106, P-ISSN 2347 - 5161

Available at http://inpressco.com/category/ijcet

Research Article

Synthesis of Silver Nanoparticles: Green Route, Antimicrobial Efficacy

B. Ajitha[Å *], Y. Ashok Kumar Reddy[Å] and P. Sreedhara Reddy[Å]

[Å]Department of Physics, Sri Venkateswara University, Tirupati-517502, Andhra Pradesh, India

Accepted 10 January 2014, Available online 01 February 2014, **Special Issue-2, (February 2014)**

Abstract

Silver nanoparticles (Ag NPs) have been synthesized by a facile green method, in which the nanoparticles are yielded in just a few minutes with long-term stability. Silver ions are reduced by means of Abrus precatorius leaf extract (LE), which acts as both reductant and stabilizer concurrently for Ag NPs preparation. The bio-reduced Ag NPs were appropriately characterized. The colorless reaction mixture turned yellow and displayed UV–Vis spectra with surface plasmon resonance at 420 nm typical for Ag NPs. The crystalline nature of NPs was evidenced by both XRD and SAED patterns. The results demonstrate the formation of crystalline Ag NPs with fcc structure having an average crystallite size of 12 nm from XRD profile. Obtained Ag NPs exhibited photoluminescence with E_x of 370 nm. Fourier infrared spectroscopy (FTIR) indicated the role of different functional groups in the Ag NPs formation. Antimicrobial activity was carried out against different test pathogens, in which more inhibitory activity was showed towards Pseudomonas spp. and Penicillium spp. with respect to antibacterial and antifungal properties.

Keywords: *Silver nanoparticles, Green route, Abrus precatorius, Leaf extract, Antimicrobial activity.*

1. Introduction

Nanotechnology is burgeoning day by day with predominant importance in an utmost level due to its new out comings in the present scenario. It has owned a prestigious premier position having significant focus in present research field which controls matter on the atomic and molecular scale resulting in enhancing new spectrum of applications in wide range. The interest on noble metal nanoparticles stems from their unique optical (Prashant, *et al*, 2008), electronic (Lim, *et al*, 2006) and catalytic (Kohler, *et al*, 2008) properties, which are different from their bulk counterparts and hence lead to novel applications. In general nanoparticles can be prepared by several methods via photochemical (Li, *et al*, 2005), chemical reduction (Wang, *et al*, 2005), γ-radiation (Choi, *et al*, 2005) and heat evaporation (Smetana, *et al*, 2005) etc. Previous studies have shown that experimental conditions, the kinetics of the interaction between metal ions and reducing agents and the stabilization processes of metal nanoparticles which influences the size, morphology, stability and the chemico–physical properties of the metal nanoparticles (Knoll and Keilmann, 1999), (Sengupta, *et al*, 2005). Hence, prerequisite design of the synthesis method where there is a feasibility of controlling size, morphology, stability and properties of metal nanoparticles has become a major concern.

Among nanoparticles, nanosilver has found tremendous applications such as biosensing, imaging, drug delivery, antimicrobials, therapeutics, catalysis and in medicine (Nair and Laurencin, 2007), (Lee and El-Sayed, 2006), (Rai, *et al*, 2009), (Claus and Hofmeister, 1999). Chemical reduction is the mostly applied method for the preparation of Ag NPs. But, chemical synthesis method lead to presence of some toxic chemicals absorbed on the surface of metal NPs which limit their usage in medical applications. Hence, there is a need for economic, commercially viable as well as environmentally clean synthesis route to prepare silver nanoparticles.

The development of new "green chemistry" synthetic processes using eco-friendly solvents and renewable, nontoxic starting materials and reagents is highly desirable taking into account the increasing interest in the total elimination, or at least the minimization of waste and chemicals toxicity and the implementation of sustainable processes. Green synthesis provides advancement over chemical and physical methods as it is cost effective, environment friendly and easily scaled up for large scale synthesis. The green synthesis of Ag NPs includes three main steps based on green chemistry perspectives i.e., i) solvent medium selection, ii) selection of eco-friendly reducing agent and iii) choosing nontoxic substances for the stability of nanoparticles. Therefore, the biosynthesis of Ag NPs through green chemistry via chemical reduction has been explored.

In our present study, we describe the biosynthesis of Ag NPs using the naturally available *Abrus precatorius* leaf as a biomaterial. *A. precatorius*, a popular medicinal plant also known as jequirity bean belongs to *Fabaceae* family. The plant is a climbing vine indigenous in India and Indonesia. Many medicinal uses are ascribed to this plant. But, *A. precatorius* beans (seeds) with attractive

*Corresponding author: **B. Ajitha**

scarlet color are more poisonous under the toxic plant parts worldwide due to the presence of toxic glycoproteins and abrin. Despite the known toxicity of *A. precatorius* seeds, their roots and leaves have been used as a substitute for licorice root, the source of the sweet oleanane-type triterpine glycoside, glycyrrhizin (Dymock, *et al*, 1890), (Hooper, 1894), (Morton, 1891). However, leaves are sweeter than roots and they have described as equivalent in sweetness potency to sucrose (Dymock, *et al*, 1890), (Hooper, 1894). In the Ayurvedic medicine, leaves of *A. precatorius* are used as aphrodisiac, tonic, remove biliousness, useful in eye diseases, cures leucoderma, itching, skin diseases, flu, inflammation and wounds. In addition Leaves are used as substitutes for licorice (mulethi) considered useful in biliousness and in leucoderma, itching and other skin diseases (Mistry, *et al*, 2010). Previous report shows that *A. precatorius* leaves can be used by people for the treatment of epilepsy (Moshi, *et al*, 2005).

The phyto-constituents of aqueous extract of *A. precatorius* leaf include tannins, saponins, flavonoids, reducing sugar, total glycosides, cardiac glycosides, proteins, triterpines, carbohydrates and alkaloids (Seganuwan and Onyeli, 2012). The leaf extract of *A. precatorius* exhibits antioxidant, anti-proliferative, anticancer, antidiabetic, antimicrobial, hepato-protective, neuroprotective and antiplasmoidal activities due to the synergistic actions of bioactive compounds such as polyphenols and flavonoids present in them (Dixon, *et al*, 2005), (Manian, *et al*, 2008), (Gul, *et al*, 2013), (Saganuwan, *et al*, 2011). The phytochemicals of leaf extract are believed to play an important role in biological activities.

Here in, to the best of our knowledge, we report for the first time synthesis of silver nanoparticles, reducing the silver ions by the aqueous extract of *A. precatorius* leaf. Further these biologically synthesized nanoparticles were evaluated for their antibacterial and antifungal properties against different pathogenic bacteria and fungi.

2. Experimental

2.1 Materials

Silver nitrate ($AgNO_3$) was purchased from Sigma-Aldrich with ≥ 99.5% purity from India. Fresh leaves of *Abrus precatorius* have been cropped from in and around Chittoor district, A.P, India. Milli-Q water was used throughout the experiment.

2.2 Preparation of leaf extract

The fresh plant material leaves of *A. precatorius* were used for the preparation of leaf extract (LE). The leaf was cut into small pieces and thoroughly surface washed at first with running tap water followed by Milli-Q water. Then leaves were shade dried for 5 days to completely remove the moisture from leaves and pulverized with the help of motor and pestle to obtain a fine powder. The leaf powder (10 g) was weighted and added to 100 ml of Milli-Q water in a conical flask and heated at 60^{o}C for 15 min. Then after extracts were filtered through Whatman No.1 filter paper followed by removal of residue and storage of filtered extract at room temperature for further experiments.

2.3 Synthesis of silver nanoparticles

For the synthesis of Ag NPs, 50 ml of 0.001 M $AgNO_3$ solution was first prepared in an Erlenmeyer flask of 100 ml volume then 10 ml of aqueous extract of *Abrus precatorius* was added and mixed thoroughly using magnetic stirrer. A control setup was also maintained with pure leaf extract. The reaction mixture (leaf extract + $AgNO_3$ solution) was then, heated at 60^{o}C under continuous stirring for 5 min and the solution turns to yellowish color indicating the formation of silver nanoparticles (Fig.1). At last the colloid solution was transferred into an amber bottle and stored at room temperature. The obtained Ag NPs solution was further purified by repeated centrifugation at 10,000 rpm for 15 min followed by re-suspension of the pellet in Milli-Q water. To avoid the photo inactivation of silver nitrate the whole experiment was carried out in dark room.

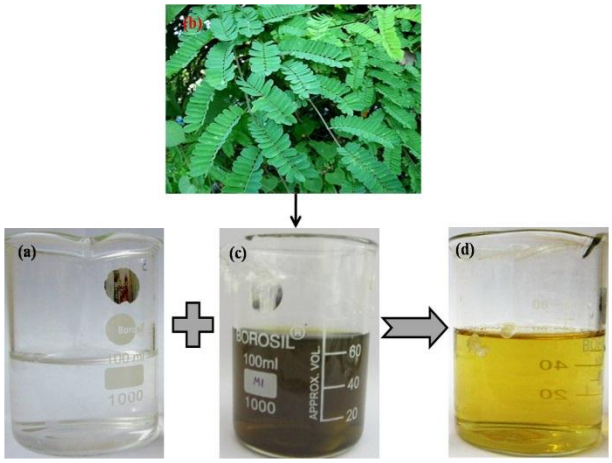

Fig.1 Schematic synthesis procedure of green silver nanoparticles (a) $AgNO_3$ solution, (b) collected *Abrus precatorius* leaves, (c) solution of leaf extract and (d) biosynthesized Ag NPs solution

2.4 Characterization of the synthesized Ag NPs

The bio-synthesized Ag NPs were characterized by various instrumental analyses. Crystalline metallic silver was examined by Seifert 3003TT X-ray diffractometer, using Cu Kα radiation (λ=0.1546 nm). Elemental compositional studies were investigated through energy dispersive spectroscopy (EDS) by using Oxford Inca Penta FET x3 EDS instrument coupled with Carl Zeiss EVO MA 15 scanning electron microscopy. The morphology of bio-reduced Ag NPs was observed using a ZEISS, SUPRA 55 field emission scanning electron microscopy (FESEM) measurements. The particle size and structure confirmations were analysed by Phillips TECHNAI FE 12, transmission electron microscopy (TEM). UV-Vis absorption studies were carried out by a Perkin Elmer

Lambda 950 UV-Vis-NIR spectrophotometer with a wavelength resolution better than ±0.2 nm. Photo-luminescence spectrum was recorded using Horiba Jobin-Yvon Fluorolog-3 Spectrofluorometer (Model FL3-22PTI). Fourier transform infrared spectroscopy (FTIR) spectrum of the freeze-dried sample was recorded with ATR-FTIR using Bruker Vertex-80 spectrometer. All the measurements were done at room temperature.

2.5 Antibacterial experiment

The bio-synthesized silver nanoparticles are tested for antibacterial activity by standard Kirby-Bauer disc diffusion method against the gram-negative (*Escherichia coli, Pseudomonas spp*.) and gram-positive (*Bacillus spp., Staphylococcus spp*.) test pathogens. The bacterial test pathogenic organisms were maintained in nutrient broth for 24 h and kept undisturbed until required for use. Nutrient agar plates were prepared containing peptone (0.5%), yeast extract (0.2%), sodium chloride (0.5%) and agar (1.5%) per liter of distilled water, sterilized and left for solidification. Then 24 h activated bacterial cultures of respective organisms were spread over the nutrient agar using a sterile glass rod to acquire bacterial lawns. Double sterilized paper discs were prepared with Whatman No.1 filter paper (diameter of ~ 4 mm) and kept on agar plates followed by Ag NPs loading on to each disc at specific concentrations of 2 µl, 4 µl, 6 µl, 8 µl and incubated at 37^{o}C for 24 hrs. Fruitful test results were scored when zone of inhibition was observed around each disc after the incubation period confirming bactericidal property of Ag NPs.

2.6 Antifungal experiment

Fungicidal properties of Ag NPs were studied towards fungal test cultures include *Aspergillus niger, Aspergillus flavus and Penicillium spp.* through disc diffusion method. The pathogenic test fungi were grown in potato dextrose broth (PDB) for 72 h and utilized at required conditions. The fungal test lawn cultures are obtained through pour plate method using (200 µl) of corresponding suspensions on potato dextrose agar (PDA) media with the help of a spreader. The discs were prepared with Whatman No. 1 filter paper (diameter of ~ 4 mm) and then placed on PDA petriplates. Finally Ag NPs were loaded onto each disc at required concentrations of 2 µl, 4 µl, 6 µl and 8 µl respectively and plates were subjected to incubation for 72 h at room temperature. Positive test results were scored when clear zone was observed around each disc after incubation period demonstrating fungicidal properties of Ag NPs. The diameter of all such zones was measured using a meter ruler and mean values for each organism were recorded and represented in millimeters.

3. Results and discussion

3.1 Structural analysis

Crystalline nature of the purified Ag NPs was evaluated using powder XRD. Fig.2 shows XRD profile of Ag NPs with four discrete diffraction peaks at 2θ=38.1, 44.2, 64.4 and 77.3 in the whole spectrum of 2θ value ranging from 20 to 80^{o} which correspond to (111), (200), (220) and (311) facets of face-centered cubic (fcc) of silver respectively (JCPDS No. 04-0873). The (200), (220) and (311) lattice planes are less intense, relative to the intense (111) plane. Thus, conforming (111) as a preferential orientation and Ag NPs are expected to have more (111) facets. This feature indicates that the nanocrystals are highly anisotropic (Priyadarshini, *et al*, 2013). Broadened peaks represent particles in nanorange. Absence of other peaks reveals the purity of Ag NPs.

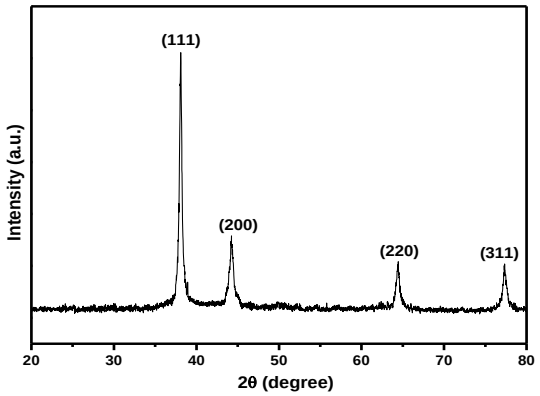

Fig.2 X-ray diffraction profile of bio-synthesized Ag NPs using *A. precatorius* leaf extract

Table 1 The variation of interplanar spacing, lattice parameter, FWHM and crystallite size values of Ag NPs using *A. precatorius* leaf extract.

Plane (hkl)	Interplanar spacing (nm)	Lattice parameter (nm)	FWHM (rad)	Crystallite size (nm)
(111)	0.235	0.408(6)	0.011	13.9
(200)	0.204	0.409(1)	0.016	9.7
(220)	0.144	0.408(3)	0.019	9.0
(311)	0.123	0.408(7)	0.013	14.2

The mean crystallite size (D) of the Ag NPs formed in the reduction process is estimated to be 12 nm, by using Scherrer's equation (Cullity, 1978),

$$D = K\lambda/\beta\cos\theta \quad (1)$$

where K denotes the shape dependent Scherrer's constant (K=0.94), λ X-ray wavelength (0.1546 nm), β full-width at half-maximum of diffraction line in radian and θ half diffraction angle. The interplanar spacing, lattice parameters, FWHM and crystallite sizes of all facets are determined and listed in Table 1 and the average particle size was found to be 12 nm.

3.2. Compositional analysis

Elemental composition information of Ag NPs was carried by EDS analysis and is depicted in Fig.3(a). EDS spectrum confirms the presence of strong elemental signal of the silver approximately at 3 keV which is typical for the absorption of metallic silver nanocrystallites due to surface plasmon resonance (Kalimuthu, *et al*, 2008).

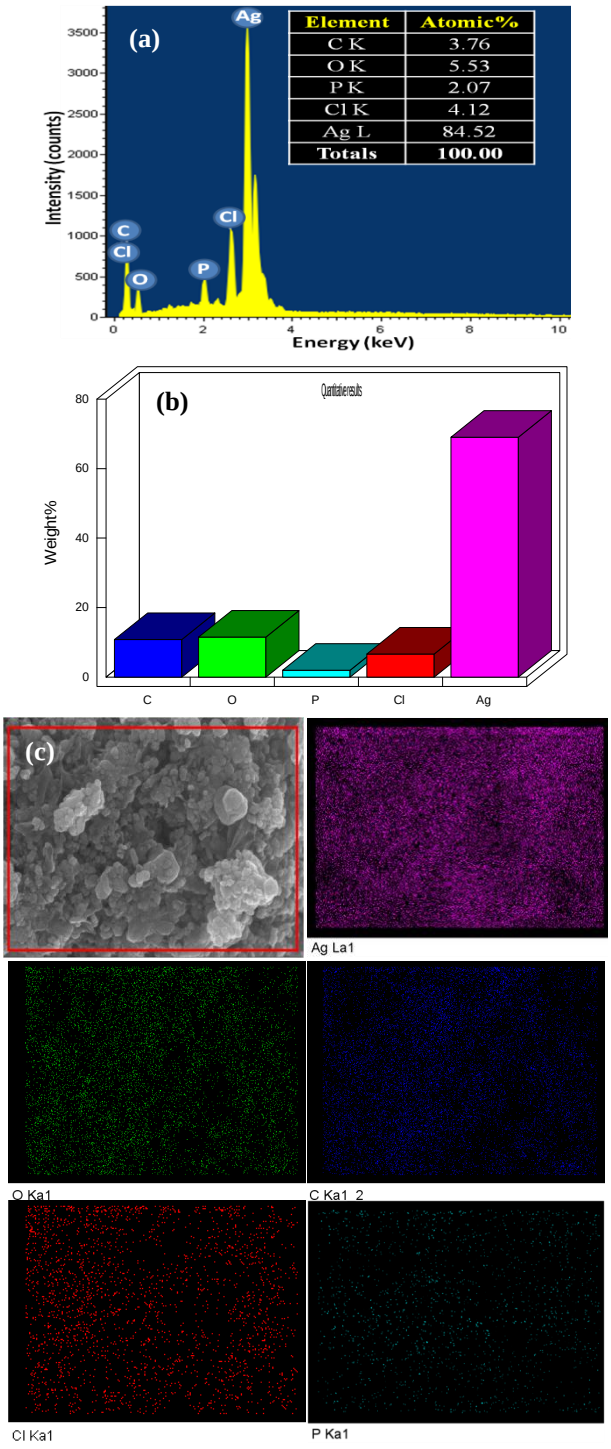

Fig.3 (a) EDS spectrum, (b) Quantitative analysis and (c) Selected area elemental mapping of synthesized Ag NPs using *A. precatorius* leaf extract

Identification lines for major emission energies of silver were displayed and are in accordance with peaks in the spectrum. Along with Ag peak, the C, O, P and Cl peaks were appeared with lower intensity due to the presence of biomolecules of leaf extract and which are bound to the surface of the Ag NPs resulting in the NPs formation.

Fig.3(b) and 3(c) displays quantitative information and the selected area elemental mapping of the green synthesized Ag NPs. Quantitative analysis suggested that Ag, O, C, Cl and P elements exhibited weight percentages of 78.3%, 8.3%, 8.1%, 4.1% and 1.2% respectively. From the selected area elemental mapping, it is pertinent to note that Ag, O, C, Cl and P elements were present uniformly throughout the sample in homogeneous manner.

3.3 Morphological studies

The topographic features of biosynthesized Ag NPs were analyzed in order to evaluate the size, shape and morphology using FESEM and TEM analysis. FESEM images at different magnifications are shown in Fig.4(a, b). The nanoparticles predominately adopt a near spherical morphology with somewhat aggregation and average particles size of 20 nm (Fig.4).

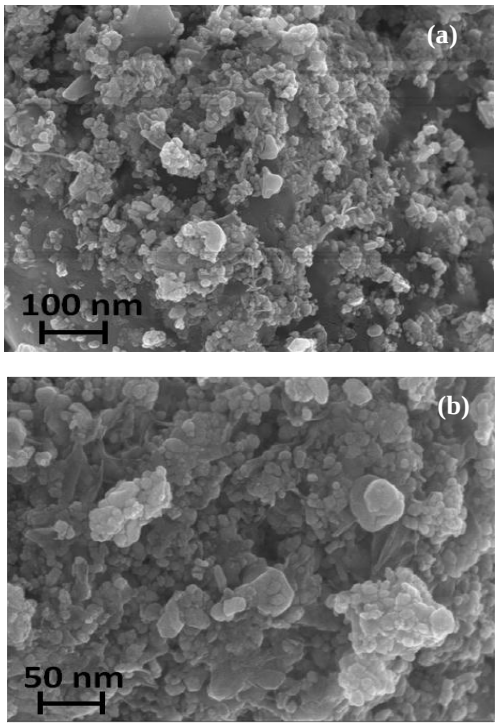

Fig.4 FESEM images (a, b) of biosynthesized silver nanoparticles at different magnifications

Fig.5(a) shows TEM image of bio-reduced Ag NPs. TEM measurements also confirm the formation of nearly spherical nanoparticles with average particle size of 14 nm. In rare occasions, particles with higher size were also seemed in the sample but their population was rather low. The selected area electron diffraction (SAED) pattern of Ag NPs is pictured in Fig.5(b), showed five strong fringes (111), (200), (220), (311) and (222) which are relevant to the characteristic peaks of face centered cubic crystalline structure evidenced by XRD results.

3.4 Optical properties

In general UV-Vis spectroscopy is a valuable tool to examine size and shape controlled nanoparticles in aqueous suspensions. The Ag NPs production was monitored with the color change through visual observation and UV-Vis spectroscopy.

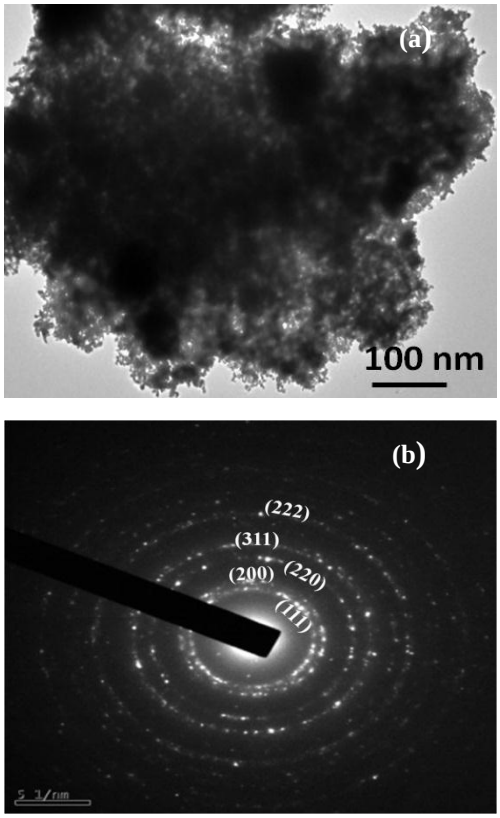

Fig.5 (a) TEM image and (b) SAED pattern of silver nanoparticles using *A. precatorius* leaf extract

The color change to yellowish brown is attributed to the collective oscillation of free conduction electrons induced by an interacting electromagnetic field in metal nanoparticles called as surface plasmon resonance (SPR), typical for Ag NPs formation. The UV-Vis spectra of formed bio-reduced Ag NPs and leaf extract are shown in Fig.6. Mie theory suggests that deviation from spherical symmetry leads to a broadening and red shift of longitudinal plasmon resonance along with appearance of transverse plasmon resonance (Mie, 1908).

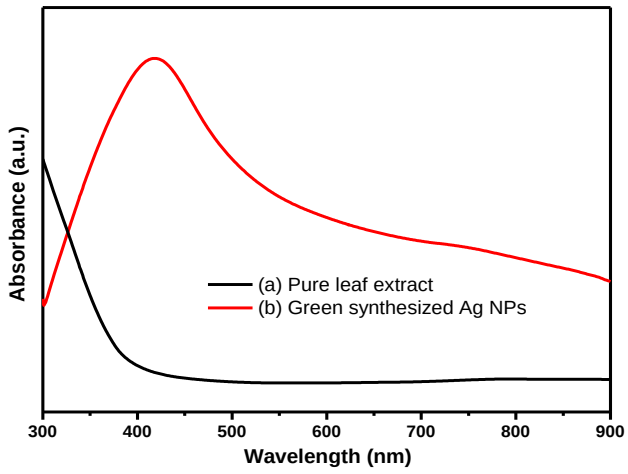

Fig.6 UV-Vis absorbance spectrum of (a) leaf extract and (b) green synthesized Ag NPs

Thus, depending on size and shape anisotropy, nanoparticles are expected to exhibit one or more SP bands: single SP band for spherical smaller ones, whereas 2 or 3 SP bands at longer wavelengths for large anisotropic particles. Therefore, absorption band at 420 nm is merely due to small spherical nanoparticles formation. No absorption peak was observed for control one (aqueous LE).

Green synthesized Ag NPs were found to be photoluminescent at room temperature. The visible luminescence of silver is due to the excitation of electrons from occupied *d* bands into states above the Fermi level then, electron-phonon and hole-phonon scattering process takes place results in energy loss and finally photoluminescent radiative recombination of an electron from an occupied *sp* band with the hole (Zhao, *et al*, 2006), (Lin, *et al*, 2007). Photoluminescence spectrum of green synthesized Ag NPs is shown in Fig.7. The sample was excited with 370 nm wavelength. From this spectrum, we observed the maximum intensity at 425 nm attributing to luminescence property.

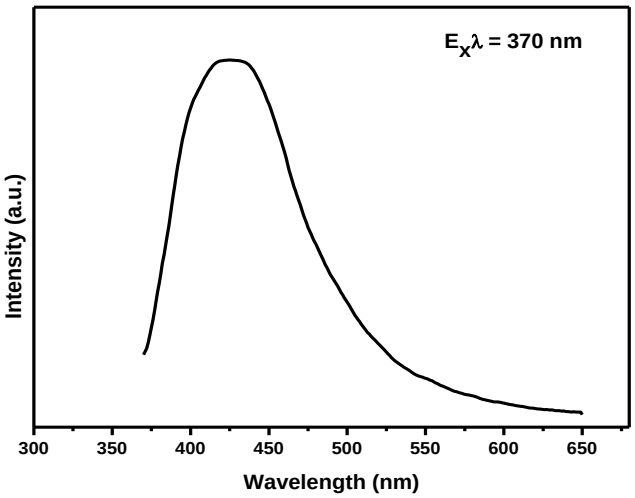

Fig.7 Photoluminescence spectra of green synthesized Ag NPs at 370 nm excitation wavelength

3.5 FTIR studies

FTIR analysis was carried out to identify the possible biomolecules present in the LE of *A. precatorius* which is exploited as reducing and capping agents for nanoparticles formation. Prominent IR bands are observed at 674, 962, 1227, 1381, 1451, 1531, 1644, 1786, 2308 and 2353 cm^{-1} (Fig.8). Most of the IR bands are characteristic of flavonoids, phenols, alkenes and carboxylate groups present in the LE. The peak at 674 cm^{-1} attributes to C-Cl stretching modes of alkyl halides. A strong band at 960 cm^{-1} corresponds to the stretching vibrations of C-O-CH_3 and -OH bending of carboxylic acids (Gunasekaran and Ponnusamy, 2005). Another strong band at 1644 cm^{-1} is recognized, related to the carbonyl stretching vibration in the amide-I linkages of the proteins (Narayanan and Sakthivel, 2011).

In phenols, in-plane bending vibration of hydroxyl groups is always centered at 1227 cm^{-1} (Gunasekaran and Ponnusamy, 2005). Peaks at 2308, 2353 cm^{-1} are assigned

to -OH stretching involved in P-OH and peaks at 1531 and 1381 cm^{-1} are characteristic of COO- (carboxylate group) asymmetric and symmetric stretching respectively (Zatihanani, *et al*, 2011). Small peak at 1786 cm^{-1} may arise from carbonyl groups of side chains of amino acids (Barth, 2000). Presence of antioxidants especially polyphenols and flavonoids in the leaf extract (Manian, *et al*, 2008), (Gul, *et al*, 2013) have recently been ascribed to have resilient antioxidant activity due to their redox properties, which enable them to act as reducing agents, hydrogen donors and singlet oxygen quenchers (Zheng and Wang, 2001), (Heck and Mejia, 2007). Hence, it may be considered that these biomolecules apart from reduction process, found to form a layer covering the Ag NPs to avoid agglomeration and thereby Ag NPs stabilization.

3.6 Antimicrobial assay

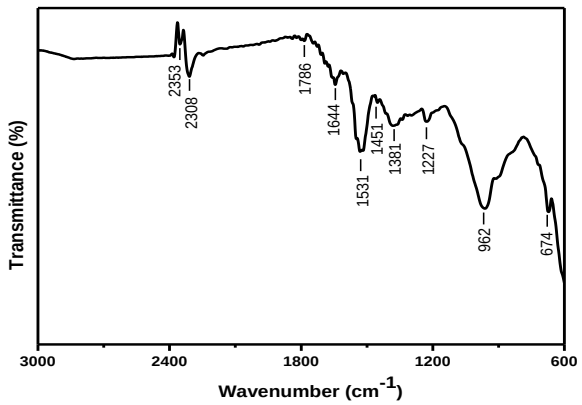

Fig.8 FTIR spectrum of green synthesized silver nanoparticles using *A. precatorius* leaf extract

In our present study, the Ag NPs synthesized using *A. precatorius* LE exerted a fairly significant antibacterial action on the tested bacteria. Fig.9 shows the zones of inhibition of *Pseudomonas spp.* and *E. coli*. *Pseudomonas spp.* depicted the highest sensitivity to nanoparticles compared to other organisms and was more adversely affected by Ag NPs that were observed from the inhibition zone in disc diffusion method. Next to this, *Staphylococcus spp.* and *Bacillus spp.* were inhibited by Ag NPs. A very small but noticeable zone of inhibition was observed for *E. coli.* This symbolizes the potentiality of Ag NPs as an antibacterial agent. It is evident by the values of diameter of zone of inhibition obtained during assessment of antibacterial activity (Table 2).

Table 2 The variation of zone of inhibitions towards different pathogenic bacteria as a function of bio-silver concentrations

Ag NPs (µl)	Zone of inhibition of tested pathogenic bacterium (mm)			
	E. coli	*Staphyloc-occus spp.*	*Bacillus spp.*	*Pseudomonas spp.*
2	5	6	5	7
4	5	7	6	8
6	6	7	7	8
8	6	7	7	9

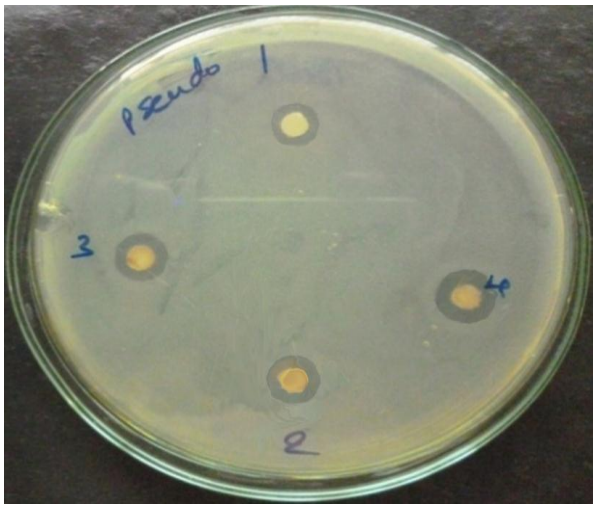

Fig.9 Disc diffusion assay of bactericidal activity against bacterial organisms at different concentrations of Ag NPs

Antifungal assay elicits that *Penicillium spp.* exhibited higher sensitivity against green biogenic Ag NPs compared to *Aspergillus niger*, *Aspergillus flavus* and *Rhizopus spp.* Among all, *Rhizopus spp.* shows lowest activity. Thus, the obtained results lend strong evidence that could warrant the consideration of Ag NPs as anti microbial agent. The Ag NPs displayed anti fungal activity towards the tested pathogenic fungi, shown in Fig.10. Zone of inhibitions of all pathogenic tested fungi are listed in Table 3.

Table 3 The variation of zone of inhibitions against different pathogenic fungi as a function of Ag NPs concentrations

Ag NPs (µl)	Zone of inhibition of tested pathogenic fungi (mm)			
	Penicillium spp.	*Aspergillus niger*	*Aspergillus flavus*	*Rhizopus spp.*
2	3	3	3	3
4	4	4	3	3
6	5	4	4	4
8	6	5	5	4

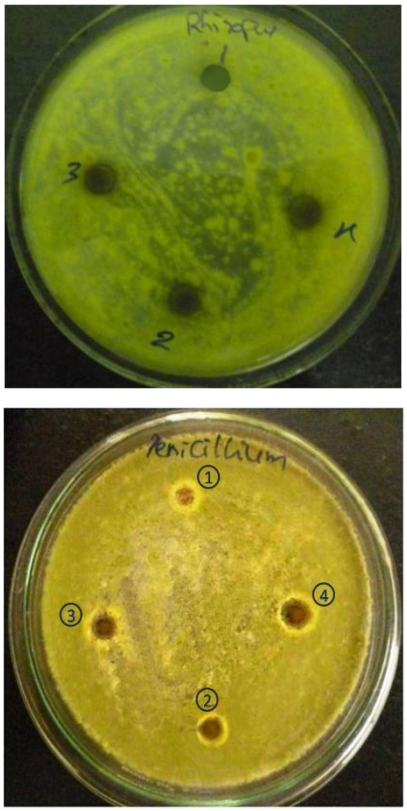

Fig.10 Disc diffusion assay of fungicidal activity against fungal organisms at different concentrations of Ag NPs

Conclusions

We have developed a fast, eco-friendly and convenient method for the synthesis of silver nanoparticles from *A. precatorius* LE. These particles are monodispersed and nearly spherical. In this green protocol, no chemical reagent or surfactant template was used. Colour change was observed due to SPR during the reaction with the LE ingredients results in formation of Ag NPs which is confirmed by UV-Vis studies. Through TEM measurements, average particles size was found to be 14 nm. From a technological point of view, these obtained Ag NPs have potential applications in the biomedical field and this simple method has numerous advantages such as low cost, elimination of chemicals toxicity, compatibility in medical applications, as well as large scale production. Finally, we concluded that antimicrobial activity of bio-reduced Ag NPs provide hope that they can be used as a potential promising antimicrobial agent.

Acknowledgements

One of the authors Ms. B. Ajitha would like to gratefully acknowledge the University Grants Commission (UGC), New Delhi, for awarding UGC-BSR Fellowship in sciences for meritorious students.

References

K.J. Prashant, H. Xiaohua, H.E. Ivan, A.E. Mostafa, (2008), Noble metals on the nanoscale: optical and photo thermal properties and some applications in imaging, sensing, biology and medicine, *Accounts of Chemical Research*, 41, 1578-1586.

D.C. Lim, I.L. Salido, R. Dietsche, M. Bubek, Y.D. Kim, (2006), Electronic and chemical properties of supported Au nanoparticles, *Chemical Physics*, 330, 441-448.

J.M. Kohler, L. Abahmane, J. Wagner, J. Albert, G. Mayer, (2008), Preparation of metal nanoparticles with varied composition for catalytical applications in microreactors, *Chem Eng Sci*, 63, 5048-5055.

Z. Li, Y. Li, X.F. Qian, J. Yin, Z.K. Zhu, (2005), A simple method for selective immobilization of silver nanoparticles, *Appl Surf Sci*, 250, 109-116.

X. Wang, J. Zhuang, Q. Peng, Y. Li, (2005), A general strategy for nanocrystal synthesis, *Nature*, 437, 121-124.

S.H. Choi, Y.P. Zhang, A. Gopalan, K.P. Lee, H.D. Kang, (2005), Preparation of catalytically efficient precious metallic colloids by γ-irradiation and characterization, *Colloids Surf. A*, 256, 165-170.

A.B. Smetana, K.J. Klabunde, C.M. Sorensen, (2005), Synthesis of spherical silver nanoparticles by digestive ripening, stabilization with various agents, and their 3-D and 2-D superlattice formation, *J Colloid Interf Sci*, 284, 521-526.

B. Knoll, F. Keilmann, (1999), Near-field probing of vibrational absorption for chemical microscopy, *Nature*, 399, 134-137.

S. Sengupta, D. Eavarone, I. Capila, G.L. Zhao, N. Watson, T. Kiziltepe, (2005), Temporal targeting of tumour cells and neovasculature with a nanoscale delivery system, *Nature*, 436, 568-572.

L.S. Nair, C.T. Laurencin, (2007), Silver nanoparticles: synthesis and therapeutic applications, *J Biomed Nanotechnol*, 3, 301-316.

K.S. Lee, M.A. El-Sayed, (2006), Gold and silver nanoparticles in sensing and imaging: sensitivity of plasmon response to size, shape, and metal composition, *J Phys Chem B*, 110, 19220-19225.

M. Rai, A. Yadav, A. Gade, (2009), Silver nanoparticles as a new generation of antimicrobials, *Biotechnol Adv*, 27, 76-83.

P. Claus, H. Hofmeister, (1999), Electron microscopy and catalytic study of silver catalysts: structure sensitivity of the hydrogenation of crotonaldehyde, *J Phys Chem B*, 103, 2766-2775.

W. Dymock, C.J.H. Warden, D. Hooper, (1890), Pharmacographia Indica, *Triibner & Co.*, Vol. 1, London.

D. Hooper, (1894), Abrus Precatorius; A Chem. Examination of the Leaves and Roots, *Pharm J Trans Third Series*, 24, 937-938.

J.F. Morton, (1981), Atlas of Medicinal Plants of Middle America: Bahamas to Yucatan, *Springfield*, Illinois.

K. Mistry, M. Mehta, N. Mendpara, S. Gamit, G. Shah, (2010), Determination of antibacterial activity and MIC of Crude extract of *Abrus precatorius* L., *Advanced Biotech*, 10, 25-27.

M.J. Moshi, G.A.B. Kagashe, Z.H. Mbwam bo, (2005), Plants used to treat epilepsy by Tanzanian traditional healers, *Journal of Ethnopharmacology*, 97, 327-336.

S.A. Seganuwan, P.A. Onyeli, (2012), Haematonic and plasma expander effects of aqueous leaf extract of Abrus precatorius in Mus musculus, *Comparative Clinical pathology*, 21, 1249-1255.

R.A. Dixon, D.Y. Xie, S.B. Sharma, (2005), Proanthocyanidins-a final frontier in flavonoid research?, *New Phytol*, 165, 9-28.

R. Manian, N. Anusuya, P. Siddhuraju, S. Manian, (2008), The antioxidant activity and free radical scavenging potential of two different solvent extracts of Camellia sinensis (L.) *Food Chem*, 107, 1000-1007.

M.Z. Gul, F. Ahmad, A.K. Kondapi, I.A. Qureshi, I.A. Ghazi, (2013), Antioxidant and antiproliferative activities of Abrus precatorius leaf extracts-an in vitro study, *BMC Complementary and Alternative Medicine*,13, 1-12.

S.A. Saganuwan, P.A. Onyeyili, E.G. Ameh, E.U. Etuk, (2011), In vivo antiplasmodial activity by aqueous extract of Abrus precatorius in mice, *Rev Latinoamer Quim*, 39, 32-44.

S. Priyadarshini, V. Gopinath, N. Meera Priyadharshini, D. Mubarakali, P. Velusamy, (2013), Synthesis of anisotropic silver nanoparticles using novel strain, Bacillus flexus and its biomedical application, *Colloids Surf B*, 102, 232-237.

B.D. Cullity, (1978), Elements of X-ray diffraction, *Edison-Wesley Pub Inc*, USA.

K. Kalimuthu, R.S. Babu, D. Venkataraman, M. Bilal, S. Gurunathan, (2008), Biosynthesis of silver nanocrystals by Bacillus licheniformis, *Colloids Surf B*, 65, 150-153.

G. Mie, (1908), Beitrage zer optik truber meiden speziell kolloidaler metallosungen, *Ann Phys*, 25, 377-445.

Y. Zhao, Y. Jiang, Y. Fang, (2006), Spectroscopy property of Ag nanoparticles, *Spectrochim Acta A*, 65, 1003-1006.

A. Lin, D.H. Son, I.H. Ahn, G.H. Song, W.T. Han, (2007), Visible to infrared photoluminescence from gold nanoparticles embedded in germano-silicate glass fiber, *Opt Express*, 15, 6374-6379.

S. Gunasekaran, S. Ponnusamy, (2005), Vibrational spectra and normal coordinates analysis on an organic non-linear optical crystal-3-methoxy-4-hydroxy benzhaldehyde, *Indian J Pure Appl Phys*, 43 (2005) 838-843.
K.B. Narayanan, N. Sakthivel, (2011), Extracellular synthesis of silver nanoparticles using the leaf extract of Coleus amboinicus Lour, *Mater Res Bull*, 46, 1708-1713.

S. Zati-hanani, R. Adnan, A.F.A. Latip, C.S. Sipaut, (2011), Synthesis, characterization and thermal properties of two novel lanthanide 2,2'-biquinoline-4,4'-dicarboxylate complexes, *Sains Malaysiana*, 40(9), 999-1006.

A. Barth, (2000), The infrared absorption of amino acid side chains, *Progress in Biophysics & Molecular Biology*, 74, 141-173.

W. Zheng, S.Y. Wang, (2001), Antioxidant activity and phenolic compounds inselected herbs, *J Agr Food Chem*, 49, 5165-5170.

C.I. Heck, E.G. Mejia, (2007), Yerba mate tea (Ilex paraguariensis): a comprehensive review on chemistry, health implication, and technological consideration, *J Food Sci*, 72, 138-151.